

Dielectrophoresis of ionized gas microbubbles: Dipole reversal due to diffusive double-layer polarization

Zachary R. Gagnon and Hsueh-Chia Chang^{a)}

Center for Microfluidics and Medical Diagnostics, Department of Chemical and Biomolecular Engineering, University of Notre Dame, Notre Dame, Indiana 46556, USA

(Received 25 August 2008; accepted 28 September 2008; published online 2 December 2008)

Gas bubbles generated by electrolysis reactions are shown to exhibit anomalous induced ac dipoles and dielectrophoretic behavior that cannot be described by classical Maxwell–Wagner theory. Normal charging and screening of conducting ionized gas in the gas-phase double layer are shown to render the bubble insulating at low ac field frequencies to affect negative dielectrophoresis. This screening effect couples with dielectric polarization at high frequencies to produce no crossover frequency for small bubbles and two crossover frequencies for bubbles larger than a critical size of $40\text{ }\mu\text{m}$. A double-layer theory accurately captures the two crossover frequencies and critical bubble size behavior. © 2008 American Institute of Physics. [DOI: [10.1063/1.3002283](https://doi.org/10.1063/1.3002283)]

Electric-field-induced interfacial polarization and particle dipoles play essential roles in determining interparticle or molecular forces during colloid self-assembly and characterization of particle suspensions.¹ The classical Maxwell–Wagner (MW) theory for an induced dipole is based on dielectric and conductive polarization, but it has been found to be inadequate to describe dielectrophoresis (DEP) in electrolytes.^{2–4} Considerable evidence suggests that ionic flux in the double layer, which is omitted in the MW theory, is responsible for such discrepancies. In fact, recent theoretical and molecular dynamics simulation efforts have been expended to extend the MW theory to account for induced double-layer polarization.^{5–10} Stern-layer conductance and adsorption are also known to play a role at low buffer ionic strength as they render the particles conductive.^{5,6} At high buffer ionic strengths, tangential ionic flux is expected to be the dominant polarization mechanism, as the normal surface field becomes negligible.^{6,9,10} In this letter, we focus on another induced-polarization phenomenon involving double-layer ion fluxes, perhaps the most dramatic one, which cannot be explained by classical MW theory: that dipole reversal can occur at two distinct crossover frequencies for a faradayically generated ionized gas microbubble with measured conductivity greater and permittivity values less than the surrounding medium. These induced bubble dipoles are size dependent such that bubbles below a critical diameter exhibit only negative DEP (*n*-DEP) toward a low-field region for all field frequencies; bubbles above have two crossover frequencies (ω_{co}). This is not the case for non-ionized gas bubbles.¹¹

Such bubbles are generated at a high voltage serpentine wire in contact with an electrolyte solution, as shown in Fig. 1(a). After generation, the small bubbles are immediately attracted to the gap between the serpentine wires, where the field is lowest. The bigger bubbles ($\geq 40\text{ }\mu\text{m}$), either generated by the reaction or from coalescence of smaller bubbles within the gap, are seen to migrate toward the high-field wire surface [Fig. 1(b)]. As seen in Fig. 2 for a single $40\text{ }\mu\text{m}$ bubble at 10 V_{rms} , the ionized bubble initially attracted to the field minimum in the wire gap at 10 kHz moves toward the field maximum when the first crossover frequency is reached

at 353 kHz . The bubble remains in a fixed position on the wire until the second crossover is reached at 1.78 MHz , and the bubble begins to migrate back toward the field minimum in the wire gap.

The wire in both figures serves as both a high voltage (3 kV_{rms}) ionizing gas producing electrochemical cell and a low voltage (10 V_{rms}) DEP crossover frequency measurement device. Planar serpentine wires were prepared on dielectric coated silicon substrate using conventional contact lithography techniques.¹² A high permittivity ($\epsilon_m=400$, $\sigma_m=110\text{ }\mu\text{S}/\text{cm}$) $4M$ solution of 6-aminohexanoic acid was prepared and characterized in a standard homemade capacitance cell with an electrode area of $\sim 40\text{ cm}^2$ and separation distance of $100\text{ }\mu\text{m}$ connected to an *LC* meter (Agilent 2720) (Supplementary Material).¹³ The solution was injected into the microchannel and placed in contact with the wire device. As described in previous work,¹² wire geometries in contact with zwitterion solutions are capable of sustaining extremely high voltages with minimal electrochemical reactions. A high voltage high frequency (3 kV_{rms} , 1 MHz) potential was dropped across the wire for a controlled amount of time (15–30 s) to generate a small suspension of ionized electrochemical gas bubbles. At this point some bubbles were observed to coalesce to a critical size and then migrate to the closest wire edges, while others remained less than $40\text{ }\mu\text{m}$ and were trapped in the wire gap. The voltage and the frequency were then reduced to 10 V_{rms} and 10 kHz , respec-

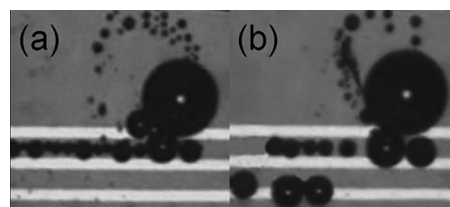


FIG. 1. (a) Suspensions of bubbles generated by electrolysis reactions by the serpentine wire. The bubbles are generated at the contact line of the big bubble resting on the electrode at 10 kHz . The small bubbles roughly $40\text{ }\mu\text{m}$ in dimension are attracted immediately to the low-field wire gap. (b) Bigger bubbles ($\sim 80\text{ }\mu\text{m}$) that form when these smaller ones coalesce in the gap or directly from the bubble source migrate toward the high-field electrode surface.

^{a)}Electronic mail: hchang@nd.edu.

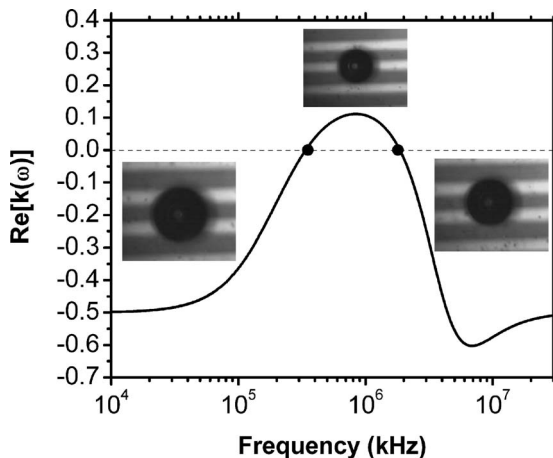


FIG. 2. The real part of the CM factor for a 65 μm bubble with a relative bubble permittivity of 30, bubble conductivity of 119 $\mu\text{S}/\text{cm}$, buffer conductivity of 110 $\mu\text{S}/\text{cm}$, and permittivity of $\epsilon_m = 400$. Experimental data were indicated as points. Insets are images of a 65 μm bubble at different frequencies.

tively, for DEP crossover frequency characterization within 30 s after generation. Upon removal of the high voltage source, rapid charge transfer from the bubble to the surrounding media was not observed. In all cases bubble crossover frequency measurements remained constant and repeatable for well over 20 min after bubble generation. It should be noted, however, that discharge was observed after approximately 45 min, as generated bubbles displayed no crossover frequency behavior, and n -DEP for all ac frequencies.

As shown in Ref. 12, the field characteristics of the serpentine wire are very different from those of conventional electrodes, as they have one large external field driven by the first and last wires and many small local fields produced by each neighboring wire pair. Therefore, it should be noted that while the generated bubble diameter in Fig. 2 is of the order of the individual wire separation length, the first and last wires which define the external polarizing field are separated by a much larger distance and sustain a field that varies weakly across one bubble. This allows the usual weak gradient approximation to be made, which leads to the DEP mobility.¹⁴ However, the existence of multiple crossover frequencies is obviously in contradiction with the classical MW theory which would predict no crossover for a less conducting bubble and one crossover for a more conducting one than the medium.

Due to the ionized state of the gas bubble, charged gas ions are free to migrate under the application of an ac electric field to form a thin charged region on the gas side interior of the bubble interface, known as the electric double layer. The time required to charge is finite and assuming a gas side double layer exists with a charging time much less than the liquid medium, n -DEP of a conductive bubble can potentially occur if one operates at a frequency that is much lower than the gas inverse charge relaxation time ($\lambda_g a/D$) ~ 350 kHz due to the insulating effect that gas side double-layer screening has on the external field. However, values higher than the inverse charge relaxation time of the gas can yield positive dielectrophoresis (p -DEP) such that the conductive polarization of gas dominates at frequencies less than the liquid side relaxation time. Finally, as one exceeds the

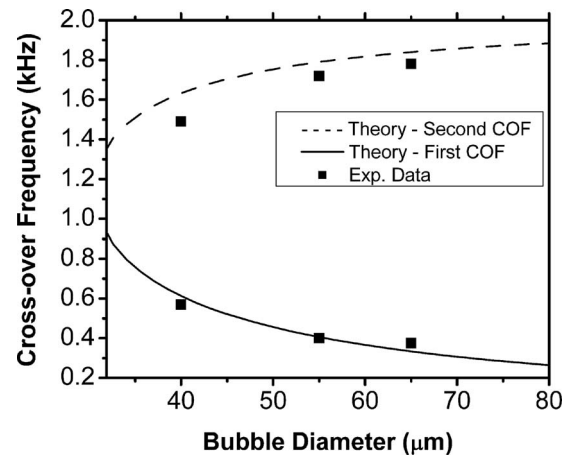


FIG. 3. The real part of f_{CM} vs bubble diameter (30–80 μm) compared to experimental data points (●) for bubble diameters of 40, 55, and 65 μm .

liquid relaxation time, gas side double-layer charging ceases and the bubble is dominated by dielectric polarization between the liquid and gas. Physically, this gas side diffusion-enhanced polarization occurs at the onset of each half-cycle when the diffusive flux due to the concentration gradient enhances charging of the counterions and discharging of the coions. Because such charging takes a finite amount of time to occur, the rate at which each half-cycle takes place determines whether the bubble will be insulating or conducting (Supplementary Material, Fig. 1). This insulating-conducting transition with respect to frequency is not exclusive. It is well known that shell-like particles such as red blood cells (RBCs) exhibit two crossover frequencies due to the thin capacitive insulating cell membrane and highly conducting cytoplasm.^{15–17} As in this work, similar to the charging mechanism of a RBC, low frequency capacitive charging renders the bubble insulating, while frequencies above the inverse relaxation time of this capacitor allow for bubble field penetration and render the bubble conductive.

To model this charging phenomenon, consider a spherical ionized conductive gas bubble exposed to an external ac field. Both the bulk electrolyte solution and the bulk gas outside their respective double layers are assumed to be electroneutral, and their potential distribution can be completely described by the Laplace equation. Due to the presence of a finite amount of charge within the diffuse part of the gas side and liquid side double layer, their potential distribution satisfies the Poisson equation. Following that of Gonzalez *et al.*⁸ for electrode double-layer polarization, one can derive two effective boundary conditions governing the charging of gas and liquid side double layers and arrive at a modified complex Clausius–Mossotti (CM) (f_{CM}) factor for an electro-neutral gas bubble with a liquid and gas side double layer (Supplementary Material),

$$f_{\text{CM}}(\omega) = \frac{f(\omega) - g(\omega) - 1}{1 - 2f(\omega) + 2g(\omega)}. \quad (6)$$

The complex functions $f(\omega)$ and $g(\omega)$ contain the permittivity ratio and charge relaxation times of the two phases. They

reduce to the dielectric polarization limit at high frequencies and the insulating bubble limit at low frequencies, with both limits exhibiting n -DEP. However, at the intermediate frequency range, the theory indeed predicts p -DEP for a sufficiently large bubble, as is consistent with the physical mechanism. As seen in Fig. 2, the theory is in quantitative agreement with the measured crossover frequencies of a 40 μm bubble. Characterization was further carried out for bubbles of diameter 40, 55, and 65 μm . As shown in Fig. 3, the critical bubble size beyond which two crossover frequencies exist with strong size dependence is also accurately captured.

Bubble interaction and mobility for bubbles with high-conductivity ionized gases are hence very different from neutral gas bubbles in an ac field due to charging and screening effects in the gas-side double layer, which can render the bubble insulating at low frequencies. This insulating effect is more pronounced for small bubbles when the bubble size approaches the gas-phase double-layer thickness. For a sufficiently small bubble, the bubble remains an insulator even at frequencies approaching the inverse dielectric polarization time scales, such that no crossover is observed.

- ¹T. Bellini, F. Mantegazza, V. Degiorgio, R. Avallone, and D. A. Saville, *Phys. Rev. Lett.* **82**, 5160 (1999).
- ²L. Gorre-Talini, S. Jeanjean, and P. Silberzan, *Phys. Rev. E* **56**, 2025 (1997).
- ³S. Tsukahara, T. Sakamoto, and H. Watarai, *Langmuir* **16**, 3866 (2000).
- ⁴N. G. Green and H. Morgan, *J. Phys. Chem. B* **103**, 41 (1999).
- ⁵I. Ermolina and H. Morgan, *J. Colloid Interface Sci.* **285**, 419 (2005).
- ⁶S. Basuray and H.-C. Chang, *Phys. Rev. E* **75**, 060501 (2007).
- ⁷E. Salonen, E. Terama, I. Vattulainen, and M. Karttunen, *Europhys. Lett.* **78**, 48004 (2007).
- ⁸A. Gonzalez, A. Ramos, N. G. Green, A. Castellanos, and H. Morgan, *Phys. Rev. E* **61**, 4019 (2000).
- ⁹S. S. Dukhin and V. N. Shilov, *Adv. Colloid Interface Sci.* **13**, 153 (1980).
- ¹⁰K. T. Chu and M. Z. Bazant, *Phys. Rev. E* **74**, 011501 (2006).
- ¹¹T. B. Jones and G. W. Bliss, *J. Appl. Phys.* **48**, 1412 (1977).
- ¹²Z. Gagnon and H.-C. Chang, *Electrophoresis* **26**, 3725 (2005).
- ¹³See EPAPS Document No. E-APPLAB-93-064842 for a detailed experimental and theoretical description. For more information on EPAPS, see <http://www.aip.org/pubservs/epaps.html>.
- ¹⁴H. A. Pohl, *Dielectrophoresis* (Cambridge University Press, Cambridge, 1978); H. Morgan and N. G. Green, *AC Electrokinetics: Colloids and Nanoparticles* (Research Studies Press, Hertfordshire, 2003).
- ¹⁵H.-C. Chang, *AIChE J.* **53**, 2486 (2007).
- ¹⁶J. Gordon, Z. Gagnon, and H.-C. Chang, *Biomicrofluidics* **1**, 044102 (2007).
- ¹⁷Z. Gagnon, J. Gordon, S. Sengupta, and H.-C. Chang, *Electrophoresis* **29**, 2272 (2008).